Proc. Natl. Acad. Sci. USA
Vol. 77, No. 5, pp. 2537–2541, May 1980
Biochemistry

Lateral mobility of band 3 in the human erythrocyte membrane studied by fluorescence photobleaching recovery: Evidence for control by cytoskeletal interactions

(lateral diffusion/spectrin)

DAVID E. GOLAN*† AND WILLIAM VEATCH*‡

*Department of Pharmacology, Harvard Medical School, Boston, Massachusetts 02115; and †Department of Molecular Biophysics and Biochemistry, Yale University School of Medicine, New Haven, Connecticut 06510

Communicated by Arthur B. Pardee, February 11, 1980

ABSTRACT **Band 3, the major intrinsic protein of the human erythrocyte membrane, was specifically labeled with the covalent fluorescent probe eosin isothiocyanate. The lateral mobility of labeled band 3 in the plane of the membrane under various conditions of ionic strength and temperature was examined by using the fluorescence photobleaching recovery technique. Low temperature (21°C) and high ionic strength (46 mM $NaPO_4$) favored immobilization of band 3 (10% mobile) as well as slow diffusion of the mobile fraction (diffusion coefficient $D = 4 \times 10^{-11}$ cm^2 sec^{-1}). Increasing temperature (37°C) and decreasing ionic strength (13 mM $NaPO_4$) led to an increase in the fraction of mobile band 3 (90% mobile) and a reversible increase in the diffusion rate of the mobile fraction ($D = 200 \times 10^{-11}$ cm^2 sec^{-1}). The increase in the fraction of mobile band 3 was markedly dissociated, however, from the increase in the diffusion rate of the mobile fraction. Thus, the fraction of mobile band 3 always increased at higher ionic strength and lower temperature than the ionic strength and temperature at which the diffusion rate increased. This dissociation was manifested kinetically on prolonged incubation of ghosts at constant ionic strength and temperature: the diffusion rate of the mobile fraction increased slowly at first and much more rapidly after the initial lag period, whereas the fraction of mobile band 3 increased almost immediately to 90% and remained maximal for the duration of the experiment. Further, changes in diffusion rate with temperature were promptly and totally reversible, whereas increases in the mobile fraction were only slowly and partially reversible. These effects were shown not to be due to complete dissociation of spectrin, the major protein of the erythrocyte cytoskeleton, from the membrane. This evidence suggests control of band 3 lateral mobility by at least two separate processes. The process that determines the diffusion coefficient of the mobile band 3 is completely reversible, and it probably involves a metastable state of cytoskeleton structure intermediate between tight binding to the membrane and complete dissociation from it.**

Extensions of the fluid-mosaic model for membrane structure (1) have emphasized the importance of intramembranous (especially transmembranous) forces in the modulation of lateral mobility of integral membrane proteins (2, 3). Immunologic phenomena such as antibody-induced patching and capping and anchorage modulation (reviewed in ref. 3) demonstrate a functional role for such forces in mammalian cell membranes. With reference to the human erythrocyte membrane, qualitative evidence for cytoskeletal control of integral membrane protein distribution and mobility has emerged from freeze-fracture electron microscopic studies (4–7). Direct examination of the lateral mobility of fluorescently labeled transmembrane proteins (chiefly band 3 and glycophorin) by the cell fusion (8) and photobleaching recovery (9) techniques has also suggested restricted mobility for these proteins.

A definitive proof of regulated mobility lies in the demonstration of reversible conditions under which such restrictions are progressively lifted. We reasoned that the same experimental parameters important in complete dissociation of the erythrocyte cytoskeleton from the membrane—i.e., low ionic strength, high temperature, and time—might also be involved in a rearrangement of cytoskeletal membrane proteins that would precede both complete cytoskeletal dissociation and frank ghost membrane vesiculation. Such a rearrangement could involve a metastable state of cytoskeleton structure, intermediate between tight binding to the membrane and complete dissociation from it, which would allow unrestricted mobility of the major integral membrane protein, band 3.

Band 3 was specifically labeled with the covalent fluorescent probe eosin isothiocyanate and its lateral mobility in the plane of the erythrocyte ghost membrane was quantitatively examined by using the fluorescence photobleaching recovery (FPR) technique (10, 11). In this technique, a single fluorescently labeled cell membrane is observed in a fluorescence microscope, using a sharply focused laser beam as the excitation source. A small area of the membrane is exposed to a brief, intense pulse of laser light, which causes irreversible photochemical bleaching of the fluorophore in that area. The rate and total amount of recovery of the fluorescence in the bleached region, which results from lateral diffusion of unbleached fluorophore into the bleached area, are monitored with a photomultiplier tube. Appropriate analysis of the fluorescence recovery curves (Fig. 1) allows estimation of: (*i*) the type of process that is leading to recovery; (*ii*) the relative amounts of mobile and immobile fluorophore; (*iii*) the lateral diffusion coefficient of the mobile fraction; and (*iv*) the presence or absence of discrete domains in the membrane comparable in size to the bleaching laser beam.

MATERIALS AND METHODS

Eosin Isothiocyanate Labeling of Band 3. The labeling procedure was taken from Cherry *et al.* (12). Briefly, washed erythrocytes from fresh human blood were mixed with eosin 5-isothiocyanate (Molecular Probes, Plano, TX) in phosphate-buffered saline, pH 7.4, for 3 hr at 21°C, lysed, and washed extensively in 5 mM $NaPO_4$/30 nM phenylmethylsulfonyl fluoride ($PhMeSO_2F$), pH 7.4, and stored up to 7 days at 4°C in 5 mM $NaPO_4$/10 mM NaN_3/30 nM $PhMeSO_2F$, pH 7.4. The amount of bound eosin was determined spectrophotometrically (13). Protein was determined by using the method of Lowry *et al.* (14). Sialic acid was determined fluorimetrically (15) after

The publication costs of this article were defrayed in part by page charge payment. This article must therefore be hereby marked "*advertisement*" in accordance with 18 U. S. C. §1734 solely to indicate this fact.

Abbreviations: FPR, fluorescence photobleaching recovery; $NaPO_4$, sodium (hydrogen) phosphate; $PhMeSO_2F$, phenylmethylsulfonyl fluoride.

‡ To whom reprint requests should be addressed.

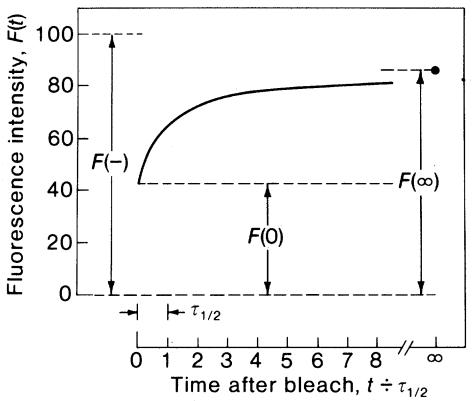

FIG. 1. Parameters involved in a typical fluorescence photobleaching recovery experiment. $F(-)$, fluorescence before bleaching; $F(0)$, fluorescence immediately after bleaching; $F(\infty)$, fluorescence long after bleaching; $\tau_{1/2}$, half-time for recovery. Diffusion coefficient $D = (w_0^2/4\tau_{1/2})\gamma_D$, in which w_0 is the $1/e^2$ radius of the Gaussian laser beam in the sample plane and γ_D is a small correction factor dependent on the magnitude of the bleaching pulse at time $t = 0$. The fractional recovery, $f(\infty) = [F(\infty) - F(0)]/[F(-) - F(0)]$, quantitates the fraction of fluorophore that is mobile—i.e., that is free to diffuse laterally with diffusion coefficient D ($cm^2\ sec^{-1}$).

sialidase treatment (16). Selectivity of labeling was assessed by $NaDodSO_4$/polyacrylamide gel electrophoresis of solubilized eosin-labeled ghosts according to Laemmli (17). Spectrodensitometric gel scans at 515 nm to monitor eosin absorbance were compared with scans of the same gels stained subsequently with Coomassie blue for protein or periodic acid–Schiff reagent for carbohydrate. Low ionic strength (18) and chloroform/methanol (19) extractions of the eosin-labeled ghosts were employed to determine quantitatively the amount of eosin label that coextracted with spectrin–actin and the sialoglycoproteins, respectively.

Sample Preparation. Eosin-labeled erythrocyte ghosts in 5 mM $NaPO_4$/10 mM NaN_3/30 nM $PhMeSO_2F$, pH 7.4 were diluted with various concentrations of $NaPO_4$ buffer, pH 7.4, and degassed in a sealed glove bag (Ventron X-27-17) by a stream of nitrogen for 3 hr at 21°C in the dark. One to 2 μl of the ghost suspension was sealed with epoxy on a microscope slide inside the glove bag. The ghost suspension spread spontaneously between the slide and cover glass, yielding a sample of average thickness 2–4 μm. This geometry oriented the 5- to 9-μm-diameter ghosts parallel to the microscope slide and maintained them in a fixed position on the microscope stage. Purging eosin-labeled ghosts of oxygen was performed to eliminate adverse photochemical crosslinking mediated by singlet oxygen (20). Control of sample temperature to within 1°C was achieved with an airstream incubator (Nicholson Precision Instruments C300) directed at the microscope stage.

FPR Measurements. The design of the optical system for FPR measurements was adapted from Jacobson *et al.* (21). A detailed description of the optics and electronics has been given (22). The size and profile of the focused laser beam in the plane of the specimen was determined by using the FPR technique itself (10). The focused laser beam was scanned with known velocity through a spot bleached in a thin (25 μm) layer of immobile fluorescein 5-isothiocyanate (Molecular Probes) embedded in resin (Sylgard 184, Dow–Corning) (23). This generated a flow recovery curve of fluorescence that showed the beam to be Gaussian in profile, with an average $1/e^2$ radius of 1.2 ± 0.3 μm ($n = 13$) in the specimen plane. Lateral mobility parameters of eosin-labeled band 3 under various conditions of ionic strength and temperature were assessed by the FPR technique (10, 11), as diagrammed in Fig. 1. Because experimental fluorescence recovery curves were found to be well fit by theoretical diffusion curves under all conditions of ionic strength and temperature (see *Results*), the data were routinely analyzed by a simple three-point fit (10) after smoothing by hand, to determine the diffusion coefficient and fractional recovery of fluorescence. At each experimental set of conditions, two to seven independent measurements (n) of lateral mobility parameters were made; the data were then expressed as mean ± SD.

RESULTS

Eosin-labeled ghosts generally had 1.1–1.7 μg of eosin bound per mg of total membrane protein, corresponding to a molar ratio of eosin to band 3 of approximately 0.75. On $NaDodSO_4$/polyacrylamide gel electrophoresis, most of the eosin absorbance was associated with band 3, with a small amount of absorbance also detected in the regions of bands 1 and 2 (data not shown). Low ionic strength treatment of eosin-labeled ghosts (which selectively releases spectrin and actin) solubilized 8 ± 2% of the total eosin along with 24 ± 6% of the total membrane protein ($n = 3$). Chloroform/methanol extraction of labeled ghosts (which selectively partitions glycophorin into the aqueous phase) resulted in the appearance of 7% of the total eosin, 5% of the total protein, and 73% of the total sialic acid in the aqueous phase. Eosin labeling was thus about 80% selective for band 3, with approximately 10% labeling of spectrin and 10% labeling of the sialoglycoproteins.

A Fraction of Band 3 Diffuses in the Plane of the Membrane. The results of a series of FPR experiments on eosin-labeled erythrocyte ghosts are summarized in Table 1. Incubation conditions ranged from 5.2 to 46 mM $NaPO_4$ buffer and from 21 to 37°C. Typical experimental recovery curves under the extremes of these incubation conditions are given in Fig. 2 and compared to theoretical FPR curves for diffusion with a Gaussian beam (10). In general the fit is excellent, implying

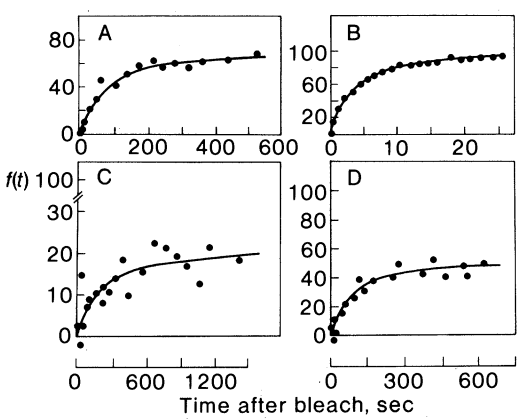

FIG. 2. Experimental FPR curves on eosin-labeled erythrocyte ghosts at the extremes of ionic strength and temperature used in this study. Theoretical curves for diffusion with a Gaussian beam were fit to the experimental points by hand. The good agreement between FPR data and theoretical curves demonstrates that lateral diffusion is responsible for the observed fluorescence recovery under all conditions of ionic strength and temperature. The parameter $f(t)$ represents the fractional recovery of fluorescence at time t; $f(t) = [F(t) - F(0)]/[F(-) - F(0)]$. Curves on left, 21°C; curves on right, 37°C. Curves at top, low ionic strength; curves at bottom, high ionic strength. Note large differences in time scale (i.e., diffusion coefficient) and fractional recovery (i.e., mobile fraction) under various conditions. (*A*) 5 mM $NaPO_4$, 21°C; $D = 6.2 \times 10^{-11}\ cm^2\ sec^{-1}$, $f(\infty) = 0.65$. (*B*) 13 mM $NaPO_4$, 37°C; $D = 130 \times 10^{-11}\ cm^2\ sec^{-1}$, $f(\infty) = 0.94$. (*C*) 46 mM $NaPO_4$, 21°C; $D = 2.1 \times 10^{-11}\ cm^2\ sec^{-1}$, $f(\infty) = 0.20$. (*D*) 46 mM $NaPO_4$, 37°C; $D = 4.4 \times 10^{-11}\ cm^2\ sec^{-1}$, $f(\infty) = 0.50$.

Table 1. Summary of FPR experiments on eosin-labeled ghost membranes[a]

$NaPO_4$,[b] mM	21°C[c] D, $cm^2\ sec^{-1} \times 10^{11}$	21°C[c] $f(\infty)$	21°C[c] n	30°C[d] D, $cm^2\ sec^{-1} \times 10^{11}$	30°C[d] $f(\infty)$	30°C[d] n	37°C[e] D, $cm^2\ sec^{-1} \times 10^{11}$	37°C[e] $f(\infty)$	37°C[e] n
5.2	5.0 ± 2.2	0.72 ± 0.07	4	11 ± 1	0.69 ± 0.08	2	—[f]	—[f]	
9.4	9.5 ± 2.3	0.51 ± 0.14	5				—[f]	—[f]	
13.3	6.7 ± 1.2	0.34 ± 0.05	3	14 ± 5	0.60 ± 0.12	4	65 ± 40	0.83 ± 0.06	3
18.8	8.7 ± 1.8	0.37 ± 0.09	3	7.9 ± 1.2	0.79 ± 0.05	3	58 ± 8	0.73 ± 0.11	2
21.4	8.2 ± 1.2	0.36 ± 0.09	6				29 ± 10	0.75 ± 0.11	7
26.0[g]	7.0 ± 3.0	0.38 ± 0.09	4	7.0 ± 3.0	0.71 ± 0.10	2	14 ± 4	0.75 ± 0.13	2
46.0	4.3 ± 2.2	0.11 ± 0.09	4				4.6 ± 0.8	0.41 ± 0.12	3

[a] $f(\infty)$ represents the fraction of band 3 molecules that is mobile—i.e., that is free to diffuse laterally with diffusion coefficient D.
[b] All samples were buffered at pH 7.4 with the $NaPO_4$ in 1 mM NaN_3/30 nM $PhMeSO_2F$.
[c] Incubation 4–5 hr, except 1–2 hr for 5.2 mM $NaPO_4$.
[d] Incubation 0.5–1 hr, except 0.25–0.5 hr for 5.2 mM $NaPO_4$.
[e] Incubation 0.5–1 hr.
[f] There was 100% ghost vesiculation.
[g] Approximate concentration.

that lateral diffusion is the only process that is contributing significantly to fluorescence recovery. The experimental data tended to be more scattered under conditions of high ionic strength and low temperature, where fractional recoveries of fluorescence were small (Fig. 2C). This was mainly a signal-to-noise problem, because the percentage contribution of noise to the experimental data was greater with smaller recovery of fluorescence intensity. Nonetheless, even under these conditions the data fit a theoretical diffusion curve well.

Diffusion Coefficient and Fractional Recovery Have Strong but Distinct Dependencies on Ionic Strength and Temperature. Low temperature (21°C) and high ionic strength (46 mM $NaPO_4$) favored immobilization of band 3 (11 ± 9% fractional recovery) as well as slow diffusion of the mobile fraction ($D = 4 \pm 2 \times 10^{-11}\ cm^2\ sec^{-1}$). Decreasing the ionic strength at this temperature caused little if any change in diffusion coefficient ($D = 5\text{–}10 \times 10^{-11}\ cm^2\ sec^{-1}$ at all phosphate concentrations) but a marked increase in the mobile fraction of band 3 [$f(\infty) = 72 \pm 7\%$ at 5 mM $NaPO_4$] (Fig. 3). At 37°C much of the band 3 was mobile even at high ionic strength (41 ± 12% fractional recovery at 46 mM $NaPO_4$), although diffusion of the mobile fraction was still slow ($5 \pm 1 \times 10^{-11}\ cm^2\ sec^{-1}$). Decreasing ionic strength at this temperature led first to a rapid increase in fractional recovery to 75 ± 13%, followed by a sharp rise in diffusion coefficient to $65 \pm 40 \times 10^{-11}\ cm^2\ sec^{-1}$ (Fig. 3). It should be noted that the sharp increase in diffusion coefficient occurred over an ionic strength range in which the fractional recovery was not changing at all. Measurement of lateral mobility at $NaPO_4$ buffer concentrations less than 10 mM at 37°C was prevented by rapid (<15 min) and total vesiculation of ghost membranes. The 1- to 2-μm-diameter vesicles produced were easily identified in the fluorescence microscope.

Increasing temperature at constant ionic strength led to increases in both diffusion coefficient and fractional recovery. These changes occurred over different ranges of ionic strength and temperature, however, and were thus dissociated from one another (Fig. 3). At 46 mM $NaPO_4$, for example, increasing temperature from 21 to 37°C caused a significant increase in the mobile fraction of band 3 (11 ± 9% to 41 ± 12%) but no change in the (still low) diffusion coefficient. Conversely, at 5.2 mM $NaPO_4$, increasing temperature from 21 to 30°C led to an increase in the diffusion coefficient (5 ± 2 to $11 \pm 1 \times 10^{-11}\ cm^2\ sec^{-1}$) but no change in the (already high) fractional recovery. At intermediate phosphate concentrations, increasing temperature resulted in an increase in fractional recovery, followed by a sharp rise in diffusion coefficient. In all cases the fractional recovery increased to 60–80% *before* the diffusion coefficient began to rise.

With Time at 37°C, Diffusion Coefficient Increases Reversibly 50-Fold Above Room Temperature Value. Under the proper conditions of ionic strength and temperature, the diffusion coefficient and fractional recovery of fluorescence were extremely sensitive to the time of incubation. Fig. 4 presents the results of an experiment in which the FPR parameters were determined every 15 min for 3 hr after the temperature of the sample had been raised from 21 to 37°C. A different cell was used for each point to avoid bleaching an area in a cell that had been bleached previously in the experiment. Within 50 min the mobile fraction of band 3 increased to a maximum value of 88 ± 10%, and it remained at that value for the duration of the

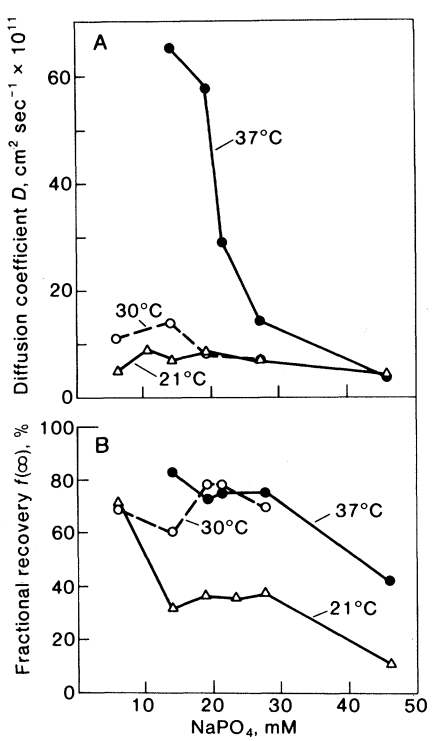

FIG. 3. Diffusion coefficients (A) and fractional recoveries of fluorescence (B) obtained from FPR experiments on eosin-labeled erythrocyte ghosts as functions of ionic strength, at various temperatures. The fractional recovery represents the fraction of band 3 molecules that is free to diffuse laterally. Each point represents the mean of two to seven independent determinations on separate ghosts (see Table 1).

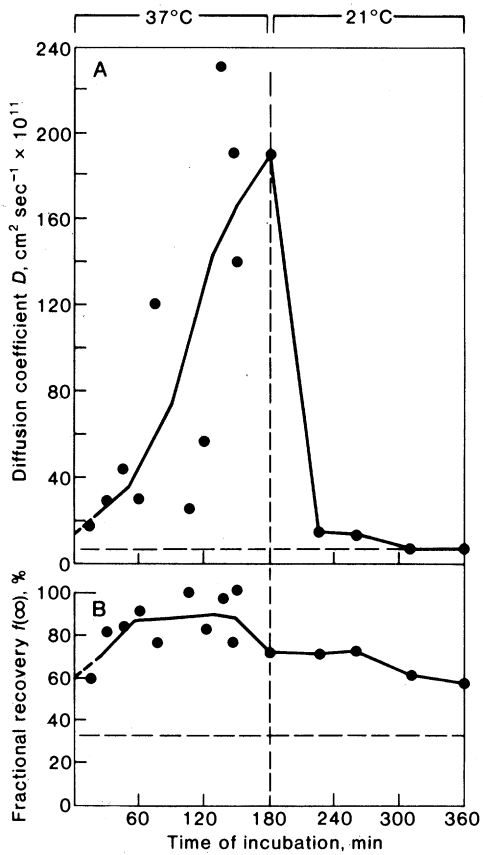

FIG. 4. Diffusion coefficients (*A*) and fractional recoveries of fluorescence (*B*) as functions of incubation time at 37°C in 13 mM $NaPO_4$ buffer. Horizontal broken lines represent initial values at 21°C, before the temperature had been increased to 37°C. Smoothed curves are drawn through the experimental points by pairwise averaging of adjacent data points. At $t = 0$, curves are extrapolated back to the values obtained at 30°C in the same buffer (probably a slight underestimate for the initial values at 37°C). The vertical broken line represents return of temperature to 21°C. Temperature equilibration time was 10–15 min. Each experimental point was obtained from a separate erythrocyte ghost in the sample.

experiment. On the other hand, the diffusion coefficient increased slowly for the first hour and much more rapidly over the following 2 hr, reaching a value of $190 \pm 30 \times 10^{-11}$ cm^2 sec^{-1} ($n = 4$) at the end of 3 hr. Lowering the incubation temperature resulted in prompt and total return of the diffusion coefficient to its initial value, but only slow and partial return of the fractional recovery.

Spectrin is Completely Dissociated at Much Lower Ionic Strengths than Those at Which Large Changes in Diffusion Coefficient Occur. The ionic strength dependence of spectrin dissociation from eosin-labeled ghosts on incubation at 37°C for 60 min is presented in Fig. 5. At $NaPO_4$ concentrations greater than 5 mM, approximately 15–20% of bands 1 and 2 were dissociated; this amount did not change with increasing ionic strength at least up to 44 mM $NaPO_4$. Below 5 mM $NaPO_4$ there was an abrupt transition in the stability of the spectrin-membrane complex, leading to 74% dissociation of spectrin at 0.1 mM $NaPO_4$. Fig. 5 also presents a comparison of the ionic strength dependence of spectrin dissociation with that of the diffusion coefficient for eosin-labeled band 3 in ghost membranes. In both cases, the ghosts were incubated at 37°C for 60 min, eliminating the effects of temperature and time from the comparison. Changes in spectrin dissociation occurred only at low ionic strengths, whereas increases in the diffusion coefficient occurred at much higher phosphate concentrations. Clearly the large increase in diffusion coefficient cannot be due to complete spectrin dissociation alone.

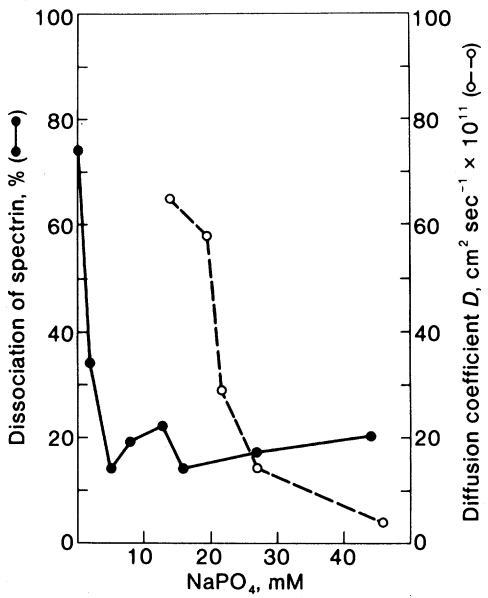

FIG. 5. Dissociation of spectrin from eosin-labeled erythrocyte ghosts with decreasing phosphate concentrations. Eosin-labeled erythrocyte ghosts were suspended in various concentrations of $NaPO_4$, pH 7.4, and incubated for 60 min at 37°C. Dissociation of spectrin from the ghost membranes was assayed as described by Bennett and Branton (24). The percent dissociation is expressed relative to a control sample maintained at 0°C in 16 mM $NaPO_4$, pH 7.4, for 60 min.

DISCUSSION

We have described a wide range of phenomena concerning the lateral mobility of band 3 in the human erythrocyte membrane. Within a fairly narrow range of temperatures (21–37°C) and ionic strengths (5–46 mM $NaPO_4$, pH 7.4), conditions were found under which reversible 50-fold changes in diffusion coefficient ($4–200 \times 10^{-11}$ cm^2 sec^{-1}) and nearly maximal changes in the mobile fraction of band 3 (10–90%) occur. Fowler and Branton (8) have also found slow (minimal diffusion coefficients $\approx 10^{-11}$ cm^2 sec^{-1}) temperature-dependent lateral mobility of erythrocyte integral membrane proteins under high ionic strength conditions. Clearly, the lateral mobility of this integral membrane protein is regulated in some organized way. From the dissociation of the ionic strength, temperature, and time dependencies of the diffusion coefficient and fractional recovery of fluorescence, it is further apparent that at least two separate processes capable of restricting band 3 lateral mobility must exist. The first process, which is only partially reversible, allows a greater and greater proportion of band 3 molecules to diffuse over large distances on the membrane. The second process, which is more difficult to set in motion than the first process but which is rapidly and totally reversible, allows the mobile fraction of band 3 molecules to diffuse much faster. The fastest lateral mobility of band 3 [$D = 190 \times 10^{-11}$ cm^2 sec^{-1}; $f(\infty) = 90\%$ at 37°C] approaches that observed for rhodopsin, an integral membrane protein that is believed to be unrestricted in the membrane (25, 26), and for lipid analogues in several natural membrane systems. This rate of diffusion may thus be reflective of completely unrestricted lateral mobility (i.e., governed only by bilayer viscosity) in the erythrocyte membrane.

Of the various mobility restraint mechanisms (2), interactions

with the erythrocyte cytoskeleton are the most likely processes controlling the lateral mobility of band 3. The involvement of mechanisms other than lipid viscosity alone is indicated by the strong ionic strength dependence of the lateral mobility parameters and by the apparent lag phase preceding the enormous rise in diffusion coefficient on increasing temperature at 13 mM $NaPO_4$. Planar aggregation of band 3 molecules must be unimportant in the control of lateral mobility, because aggregates of at least 2500 band 3 dimers would be necessary to explain a 50-fold change in diffusion coefficient (see Eq. 2 of ref. 26). The presence of domains smaller in area than about $1/4$ of the total erythrocyte membrane surface was ruled out by experiments in which bleaching laser pulses were repetitively delivered to the same area of eosin-labeled ghost membrane. Between 80 and 100% fractional recovery of fluorescence resulted consistently after the third or fourth bleach, under all conditions of ionic strength and temperature (data not shown). Had bounded domains comparable in size to the focused laser spot been present, fractional recoveries on rebleaching would never have reached these high levels (27).

Interactions between band 3 and the erythrocyte cytoskeleton could take the form of a specific ionic-strength- and temperature-dependent formation of a complex between band 3 and some immobile cytoskeletal component or a nonspecific ionic strength- and temperature-dependent entanglement of the cytoplasmic portion of band 3 in the cytoskeletal reticulum. A tight complex between band 3 and band 2.1 on the membrane has been demonstrated (28), but this could account for immobilization of at most 10–15% of the band 3. More likely candidates for interactions leading to restriction of lateral mobility are formation of a low-affinity (K_d = 1–10 μM) complex between band 3 and spectrin (see ref. 29) and high- or low-affinity binding between spectrin and other membrane elements. The latter possibilities are especially attractive, because interactions involving cytoskeletal elements are sensitive to the same parameters that affect lateral mobility strongly. Phenomena exhibiting such dependencies include spectrin elution from the membrane (5, 24), spectrin binding to inside-out vesicles (24), spectrin dimer–tetramer equilibrium (30), and susceptibility of membrane proteins to crosslinking (31). It is not difficult to imagine a relatively loose but metastable state of cytoskeleton structure intermediate between tight binding to the membrane and complete dissociation from it that would allow rapid lateral diffusion of band 3. To be consistent with our data on the reversibility of the diffusion coefficient of band 3, the postulated metastable state must be in rapid equilibrium (minutes to hours) with the tightly bound form of the cytoskeleton; this is again not unreasonable given the high affinity of at least one interaction between spectrin and the membrane (28).

Systematic study of the lateral mobility of selectively labeled membrane components by the FPR technique can provide detailed information regarding membrane structure and dynamics. In the human erythrocyte membrane system, we have presented evidence for dynamic interactions between band 3 and the erythrocyte cytoskeleton. Study of specifically labeled glycophorin mobility, as well as the effects of various exogenous and endogenous perturbants of cytoskeletal structure on the lateral mobility of band 3 and glycophorin, will further elucidate these interactions.

We thank Drs. Jon Morrow and Vincent Marchesi for helpful discussions, and Drs. Gerald Fischbach and Samuel Latt for loans of equipment. This work has been supported by U.S. Public Health Service Grant AI-15311. W.V. is the recipient of a Research Career Development Award (AI-00320). D.G. is supported by the Medical Scientist Training Program (U.S. Public Health Service Grant 5-T32-GM-07205). This work represents part of a dissertation to be presented by D.G. for the degree of Doctor of Philosophy from Yale University.

1. Singer, S. J. & Nicolson, G. L. (1972) *Science* **175,** 720–731.
2. Nicolson, G. L. (1976) *Biochim. Biophys. Acta* **457,** 57–108.
3. Edelman, G. M. (1976) *Science* **192,** 218–226.
4. Yu, J. & Branton, D. (1976) *Proc. Natl. Acad. Sci. USA* **73,** 3891–3895.
5. Elgsaeter, A. & Branton, D. (1974) *J. Cell Biol.* **63,** 1018–1030.
6. Elgsaeter, A., Shotton, D. M. & Branton, D. (1976) *Biochim. Biophys. Acta* **426,** 101–122.
7. Shotton, D., Thompson, K., Wofsy, L. & Branton, D. (1978) *J. Cell Biol.* **76,** 512–531.
8. Fowler, V. & Branton, D. (1977) *Nature (London)* **268,** 23–26.
9. Peters, R., Peters, J., Tews, K. H. & Bahr, W. (1974) *Biochim. Biophys. Acta* **367,** 282–294.
10. Axelrod, D., Koppel, D. E., Schlessinger, J., Elson, E. & Webb, W. (1976) *Biophys. J.* **16,** 1055–1069.
11. Koppel, D. E., Axelrod, D., Schlessinger, J., Elson, E. & Webb, W. (1976) *Biophys. J.* **16,** 1315–1329.
12. Cherry, R. J., Burkli, A., Busslinger, M. & Schneider, G. (1976) *Nature (London)* **263,** 389–393.
13. Cherry, R. J., Cogoli, A., Opplinger, M., Schneider, G. & Semenza, G. (1976) *Biochemistry* **15,** 3653–3656.
14. Lowry, O. H., Rosebrough, N. J., Farr, A. L. & Randall, R. J. (1951) *J. Biol. Chem.* **193,** 265–275.
15. Hammond, K. S. & Papermaster, D. S. (1976) *Anal. Biochem.* **74,** 292–297.
16. Tomita, M., Furthmayr, H. & Marchesi, V. T. (1978) *Biochemistry* **17,** 4756–4770.
17. Laemmli, U. K. (1970) *Nature (London)* **227,** 680–685.
18. Fairbanks, G., Steck, T. L. & Wallach, D. F. H. (1971) *Biochemistry* **10,** 2606–2617.
19. Hamaguchi, H. & Cleve, H. (1972) *Biochem. Biophys. Res. Commun.* **47,** 459–464.
20. Sheetz, M. P. & Koppel, D. E. (1979) *Proc. Natl. Acad. Sci. USA* **76,** 3314–3317.
21. Jacobson, K., Derzko, Z., Wu, E.-S., Hou, Y. & Poste, G. (1976) *J. Supramol. Struct.* **5,** 565–576.
22. Golan, D. E. (1979) Dissertation (Yale Univ., New Haven, CT).
23. Axelrod, D. (1979) *Biophys. J.* **26,** 557–573.
24. Bennett, V. & Branton, D. (1977) *J. Biol. Chem.* **252,** 2753–2763.
25. Edidin, M. (1974) *Annu. Rev. Biophys. Bioeng.* **3,** 179–201.
26. Poo, M.-M. & Cone, R. A. (1974) *Nature (London)* **247,** 438–441.
27. Zagyansky, Y. A. & Jard, S. (1979) *Nature (London)* **280,** 591–593.
28. Bennett, V. & Stenbuck, P. J. (1979) *Nature (London)* **280,** 468–473.
29. Bennett, V. & Stenbuck, P. J. (1979) *J. Biol. Chem.* **254,** 2533–2541.
30. Ungewickell, E. & Gratzer, W. B. (1978) *Eur. J. Biochem.* **88,** 379–385.
31. Palek, J. & Liu, S.-C. (1979) *Semin. Hematol.* **16,** 75–93.